

A NUMERICAL STUDY FOR SELF-PROPELLED JBC WITH AND WITHOUT ENERGY SAVING DEVICE

Chonghong Yin, Jianwei Wu, Tao Sun, Decheng Wan*

(State Key Laboratory of Ocean Engineering, Shanghai Jiao Tong University, Collaborative Innovation Center for
Advanced Ship and Deep-Sea Exploration, China)

*Corresponding author: dcwan@sjtu.edu.cn

1. SUMMARY

Numerical simulations are performed to study the effectiveness of the wake equalizing duct fitted on JBC. Computations of JBC with and without energy saving device are performed by the in-house multifunction solver naoe-FOAM-SJTU, which is based and developed on the open source code OpenFOAM. The solver is also implemented with dynamic overset grid that allows for arbitrary rotational speed of the propeller during the computation. Self-propulsion points are obtained in a single computation by using a controller to modify the propeller RPS until the target speed is reached. Self-propulsion factors for JBC with and without ESD are analyzed and compared with experimental data.

2. INTRODUCTION

Wake equalizing duct (WED), studied in this paper, is one of the most commonly used energy saving devices for improving the propulsion performance of a ship and reducing the propeller-excited vibrations and viscous resistance forces, especially suitable for vessels with fat stern such as bulk carrier and oil tanker. Wake equalizing duct is fitted in stern before propeller, the general function of it is set to improve uniformity of propeller's inflow field, thus homogenizing the wake and improving hull efficiency. Also, the wake equalizing duct can accelerate the flow by means of the lift created by the aerofoil shape of the duct cross-section.

There are several ways to predict the effectiveness of energy saving device, including experiments, potential theories, and computational fluid dynamics (CFD). Among them, CFD method shows a huge advantage and has gained popularity in the past decades due to a more physics-based modeling, capability of handling non-linear free-surface, especially for detail presentation of flow fields, which is important to study the effect of energy saving devices. By now, due to the complexity of the problem, most studies of energy saving devices on propulsion performance of a ship

are carried out based on model tests. Emin (2006) made a case study for the effect of a flow improvement device (a partial wake equalizing duct) on ship powering characteristics. Hansen et al (2011) evaluated the efficiency of propeller boss cap fin by model tests and sea trial. However, CFD is also becoming an effective way to overcome these complex problems, especially due to the development of dynamic overset grids. Fahri (2007) made an investigation on the wake equalizing duct of a chemical tanker by using a commercial CFD code, CFX. Shin et al. (2013) studied wake equalizing duct for self-propulsion and cavitation performances numerically and experimentally, viscous flow computations were performed using HSVA code FreSCo+ which is based on the finite-volume method.

In this paper, self-propulsion JBC models with and without wake equalizing duct are simulated and analyzed, simulations also take the effects of free surface and discretized propellers into consideration. The in-house RANS solver naoe-FOAM-SJTU is used to perform the computations, which is an upgrade version of the previous solver with dynamic overset grid capability. The solver is developed based on the open source CFD code OpenFOAM. The domain connectivity information (DCI) is generated by the Suggar library (2005) to build the connection between the overset component grids. A full 6DOF module with a body hierarchy enabling moving appendages is implemented to solve the hull motion and discretized propeller.

The paper is organized as follows. The description of computational methods is presented first, and is followed by the geometry and overset mesh. The results are then presented and discussed. Finally, a summary and conclusions are provided.

3. COMPUTATIONAL METHODS

3.1 Modeling

The computations are performed by the overset solver naoe-FOAM-SJTU. It employs the Reynolds Averaged Navier-Stokes (RANS) equations with $k-\omega$ Shear Stress transport (SST) model (2009) in the simulation of unsteady incompressible viscous two-phase flow field. The Volume of fluid (VOF) approach with an artificial compression technique is applied to capture the two-phase interface. The Finite Volume Method (FVM) (2007) is used to discretize both the RANS equations and VOF transport equation in naoe-FOAM-SJTU.

The PISO (pressure-implicit-split-operator) algorithm (2010) is adopted to solve the coupled equation of velocity and pressure. All these methodologies are provided by the original OpenFOAM library. The overset grid technique is implemented to handle the large-amplitude motion of ship and complex hierarchical motion of appendages such as rotating propeller. The overset grid method allows separate overlapping grids to move independently without restrictions. The overset approach implemented in this work requires domain connectivity information (DCI) to build the communication among separate overset grids. The Suggar library is called to generate the DCI for OpenFOAM.

3.2 Controller

A PI speed controller is applied to the propeller RPS to achieve the target speed. The error is defined as the difference between the instantaneous ship speed and the target speed.

$$e = U_{\text{target}} - U_{\text{ship}} \quad (1)$$

and the instantaneous RPS is

$$n = Pe + I \int_0^t e dt \quad (2)$$

where P and I are the proportional and integral constants of the controller.

3.3 Motions

A fully 6DOF module with hierarchy of bodies are implemented in naoe-FOAM-SJTU. This module allows ship to move independently in the computational domain and in the meanwhile, the propeller is rotating around the propeller axis. Two coordinate system, earth-fixed and ship-fixed systems are adopted in this 6DOF module. The forces and moments on ship hull and propeller are computed in earth-fixed system and then they are projected to ship-fixed system. The ship motions for the next time step are predicted by the projected forces and moments in ship fixed system. For the movements of hierarchal objects,

as shown in Fig. 1, the propeller grid rotates first about a fixed axis in the ship coordinate system, and then both ship and propeller grids translate and rotate in the earth-fixed system according to the predicted motions. At the same time, Suggar library is called to compute the DCI based on the new grid positions. OpenFOAM processors receive the new data right after the movements of the overset grids and start the computation for the next time step.

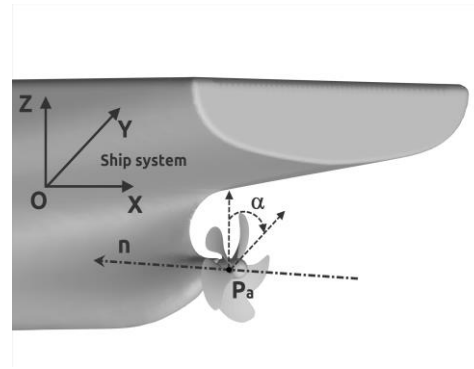


Fig.1 Demonstration of propeller rotating in the ship system

4. GEOMETRY AND MESH

4.1 JBC model

In this work, wake equalizing duct fitted in a low-speed full form ship in model scale is studied, and results of computations and investigations will be presented for resistance and propulsion. The wake equalizing duct is an effective energy saving device that have been devised especially for the ships with large block coefficients and fat stern like JBC to improve the propeller performance. The duct consists of duct and duct strut.

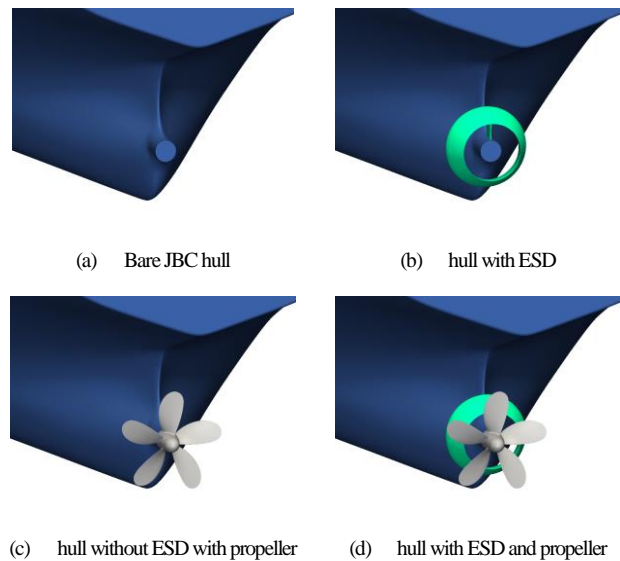


Fig.2 Computational models of JBC for resistance (a, b) and self-propulsion (c, d)

Main dimensions and particulars of JBC are listed in Table 1, including both the full scale and the model scale, and also the information regarding to position and rotation direction of propeller. The 3D models of hulls with and without wake equalizing duct are shown in Fig. 2. In order to obtain a mesh with good quality, the sides of hull deck is rounded off.

Table 1 Principle Dimensions of JBC

Main particulars	Full scale	Model scale
L_{PP} (m)	280	7
L_{WL} (m)	285	7.125
B_{WL} (m)	45	1.125
D (m)	25	0.625
T (m)	16.5	0.4125
∇ (m ³)	178369.9	2.7870
$S_{0_w/oESD}$ (m ²)	19556.1	12.2226
$S_{0_w/ESD}$ (m ²)	19633.9	12.2706
C_B	0.858	0.858
C_M	0.9981	0.9981
LCB	2.5475	2.5475
x/L_{PP}	0.985714	0.985714
$-z/L_{PP}$	-0.0404214	-0.0404214

4.2 Case conditions

Self-propulsion computations are started from the initial flow field obtained by towed calm water case. Motions are allowed only for surge, heave and pitch. In terms of the trim angle, positive value means trim by bow, and negative value means trim by stern. As the acceleration of self-propelled ship, Fr and Re numbers will increase due to the increase of the velocity on hull and propeller surfaces. Computations will evolve with the ship accelerating as the propeller impulses the ship, the PI controller is used to act on the propeller RPS to achieve the target speed. Time step is set to be 0.00025s in this computation.

JBC models were performed at $Re=7.46 \times 10^6$ and $Fr=0.142$, corresponding to a velocity of 1.179 m/s (14.5kn for full scale). To compare the numerical simulation with model test, the case conditions are set identically to the model test. The water density is 998.2 kg/m³ and the kinematic viscosity is 1.107×10^{-6} m²/s. The value of gravitational acceleration is 9.80 m/s².

4.3 Mesh and domain

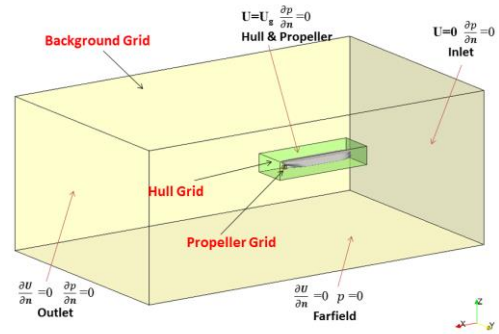
For numerical computations of self-propulsion in this paper, space coordinate range is determined as $-1.0L_{pp} < x < 4.0L_{pp}$,

$-1.5L_{pp} < y < 1.5L_{pp}$, $-1.0L_{pp} < z < 1.0L_{pp}$. The mesh is generated by SnappyHexMesh, an automatic mesh generation tool provided by OpenFOAM. The grids of important regions are refined to capture precisely the free surface, the wake flow field, and also the vortex structure. The summary of overset component grids is listed in Table 2. Boundary conditions and layout of overset grid system for self-propelled JBC are displayed in Fig. 3

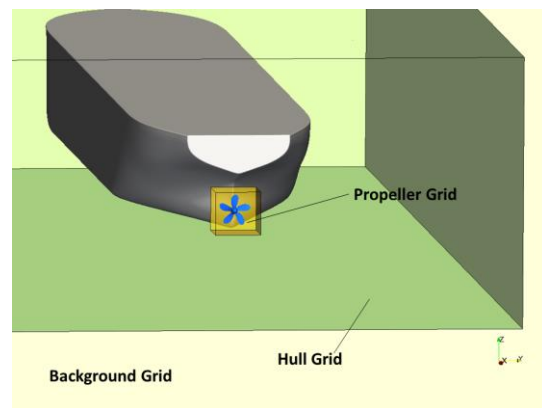
The hull uses a total of 1.42 million grids, 1.6 million while fitted with ESD. Propeller possesses the maximum amount grids of 1.9 million, and 1.41 million are used for global refinement/background grids. A small gap was left between the propeller hub and the stern hub to allow propeller rotation.

Table 2 Grid sizes of overset component grids

Grid	Hull	Propeller	Background	Total
W/O	1.42×10^6	1.90×10^6	1.41×10^6	4.73×10^6
W	1.60×10^6	1.90×10^6	1.41×10^6	4.91×10^6



(a) Overall view



(b) Stem view

Fig.3 Layout of overset grid system for self-propelled JBC

5. ANALYSIS OF RESULTS

In this part, self-propulsion computations with given SFC are performed. The ship is fitted with a five-bladed propeller denominated MP687. The rate of revolutions of the propeller n is to be adjusted by using a PI controller to obtain force equilibrium in the longitudinal direction considering the applied towing force (Skin Friction Correction, SFC). In self-propulsion cases with and without energy saving device, SFC are 18.1 N and 18.2 N respectively. Computations for self-propulsion use the same time step $\Delta t=0.00025$, the target speed in the PI controller is set to 1.179m/s, corresponding to $Fr=0.142$. The proportional and integral controller constants are set to $P=I=800$.

Resistance coefficients and self-propulsion factors are compared with experimental data in Table 3, the self-propulsion factors shown were obtained using the experimental open water curves for the MP687 propeller measured at NMRI. The total resistance coefficients from CFD computation have error about 4% compared with the experimental values. Self-propulsion factors also show excellent agreement with their corresponding experimental values with the exception of that for the hull efficiency η_H , 5.85% for hull without ESD and 5.81% for hull with ESD. ΔE is defined by equation (3):

$$\Delta E(\%) = (P_{W-ESD} - P_{WO-ESD}) / P_{WO-ESD} \times 100 \quad (3)$$

Table 3 Resistance coefficients and self-propulsion factors for self-propelled JBC with and without ESD

	EFD-W/O ESD	CFD-W/O ESD	EFD-W ESD	CFD-W ESD
$C_r(\times 10^{-3})$	4.811	4.607 (-4.24%)	4.762	4.551 (-4.43%)
K_T	0.217	0.2225 (2.55%)	0.233	0.2402 (3.07%)
$10K_Q$	0.279	0.2867 (2.76%)	0.295	0.3047 (3.30%)
$1-t$	0.8915	0.9309 (4.42%)	0.8952	0.9367 (4.63%)
$1-w$	0.5483	0.5268 (-3.92%)	0.4742	0.4480 (-5.52%)
η_o	0.4981	0.4895 (-1.72%)	0.4572	0.4446 (-2.74%)
η_R	1.0158	1.0066 (-0.91%)	1.0107	0.9929 (-1.76%)
J	0.4083	0.3983 (-2.45%)	0.3672	0.3538 (-3.64%)
n	7.8	7.682 (-1.51%)	7.5	7.354 (-1.95%)
η_H	0.8227	0.8708 (5.85%)	0.8724	0.9231 (5.81%)

- t is the thrust deduction coefficient
- w is the wake fraction coefficient
- η_o is the open water propeller efficiency
- η_R is the relative rotative efficiency
- η_H is the hull efficiency defined as $\eta_H = (1-t)/(1-w) \times \eta_o \times \eta_R$

Energy saving for self-propelled JBC with ESD is displayed in Table 4, power of the JBC propeller obtained by CFD shows great agreement with the experiment test. Propeller power P is defined as $2\pi n \times Q$, where Q is the propeller torque. The wake equalizing duct studied in this paper shows a good energy saving effect of 6.7% by CFD computation, which is 11.67% higher than the EFD value.

Also as presented in the Table 3, we can see that the wake fraction coefficient get an obvious decrease 14.9% and the hull efficiency η_H increase 5.9% after installing the wake equalizing duct, that is because the duct homogenize the wake and improve hull efficiency by accelerating the inflow to the propeller. From the decrease of resistance coefficients C_p and C_f of JBC fitted with ESD, we can see that the wake equalizing duct can also reduce the viscous resistance force by decreasing the flow separation at the stern of ship, and generating an additional thrust.

Table 4 Energy saving for JBC with ESD

		P(W)	ΔE
W/O ESD	EFD	28.621	—
	CFD	28.096 (-1.83%)	—
W ESD	EFD	26.903	6.0%
	CFD	26.200 (-2.61%)	6.7%(11.67%)

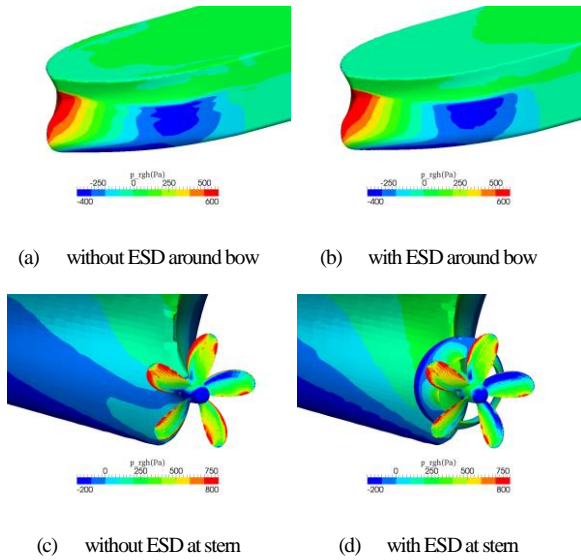


Fig.4 Pressure distribution

Fig. 4 presents the bow and stern pressure distribution of JBC with and without ESD. It shows that there is a similar pressure distribution at bow between the two ships, but due to the influence of the wake equalizing duct, stern pressure

distributions show a great difference between JBC ships with and without ESD. There is an obvious decrease of the low pressure area at the ship stern after installing energy-saving device, which can be beneficial to reduce the pressure resistance. In addition, the low pressure area created in front of the duct can also have positive effects in terms of reattaching separated flow to the hull in the vicinity of the duct. The difference of pressure distribution leads to the difference of viscous pressure resistance between JBC with and without ESD.

The simulation of vortices behind the propeller is useful to evaluate the propulsion performance. Fig. 5 shows the isosurfaces of $Q=100$ colored with axial velocity under self-propulsion conditions. Most of the vorticity is generated by the propellers. Tip vortices are well resolved in the refinement region, but only the strong hub vortex survives the transition to a coarser grid. The generation of vortex would cause a severe pressure reduction and vibration of the propeller. We can see from the figures that the propeller hub vortex structures are quite different between ships with and without ESD. Different view angles also present clearly that the propeller tip vortices and hub vortex of self-propelled JBC significantly weakened after installed the energy saving device.

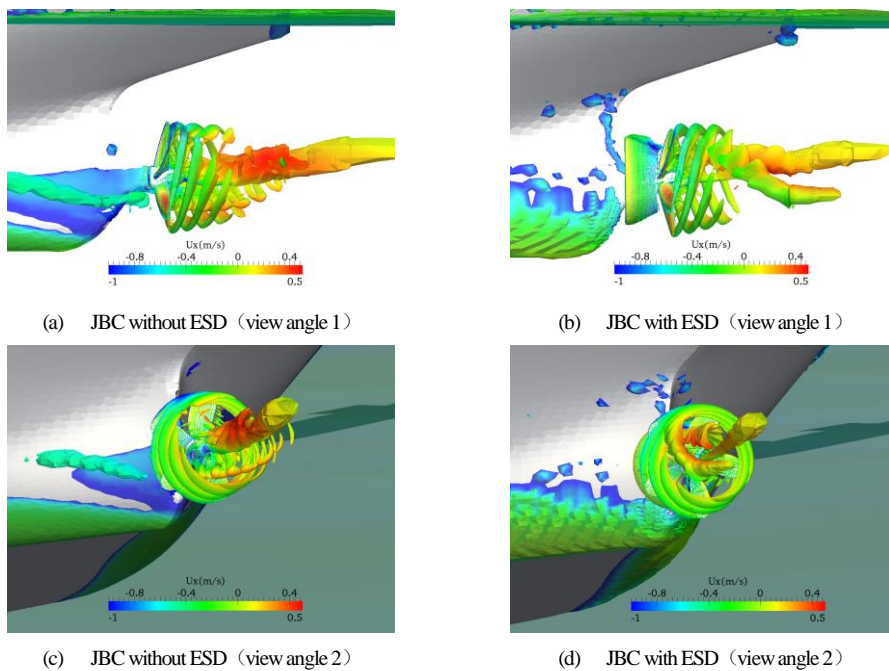


Fig.5 Isosurfaces of $Q=100$ colored according to U_x under self-propulsion

6. CONCLUSIONS

In this paper, a numerical study is carried out for studying the effectiveness of the energy saving device wake equalizing duct on JBC. Computations of self-propulsion cases with and without energy saving device are performed by the in-house multifunction solver naoe-FOAM-os-SJTU, taking free surface and direct discretized propeller into consideration. Some meaningful conclusions can be summarized.

The wake equalizing duct studied in this paper can improve the propulsion characteristics of the JAPAN Bulk Carrier considerably. It shows a good energy saving effect of 6.7% by CFD computation, which value is 6.0% according to the experimental data.

Principles of the energy saving device wake equalizing duct can be concluded as follows. Firstly, it can accelerate the flow in front of propeller disk to improve propeller's efficiency. Then, flow separation can be reduced by the duct which recovering hull surface pressure at stern. Finally, the wake equalizing duct produces additional thrust by the aerofoil shape of the duct cross-section.

The overset solver naoe-FOAM-os-SJTU is proved to be reliable to handle the propeller-hull interaction issues with viscous flow and provided detailed information of the flow fields, which is necessary for design of energy saving devices. Also, it has a good extendibility with high efficiency which will be able to solve more complex nonlinear problems.

In future work, the extensive studies including the various parameters of the wake equalizing duct can be carried out for the best propulsive performance of a specific ship hull. Also other energy saving devices need to be studied like pre-swirl duct and hub vortex absorbed fins.

7. ACKNOWLEDGEMENTS

This work is supported by National Natural Science Foundation of China (Grant Nos. 51379125, 51490675, 11432009, 51411130131), The National Key Basic Research Development Plan (973 Plan) Project of China (Grant No. 2013CB036103), High Technology of Marine Research Project of The Ministry of Industry and Information Technology of China, Chang Jiang Scholars Program (Grant No. T2014099) and the Program for Professor of Special Appointment (Eastern Scholar) at

Shanghai Institutions of Higher Learning(Grant No. 2013022), to which the authors are most grateful.

REFERENCES

- Korkut E., (2006), A case study for the effect of a flow improvement device (a partial wake equalizing duct) on ship powering characteristics. *Ocean Engineering*, 33: 205–218.
- Hansen, H. R., Dinham P., Nojiri T., (2011), Model and full scale evaluation of a propeller boss cap fin device fitted to an Aframax tanker[C]. Proceedings of the 2nd International Symposium on Marine Propulsors. Hamburg, Germany. 15–17 June.
- Fahri C., (2007), A numerical study for effectiveness of a wake equalizing duct[J]. *Ocean Engineering*, 34: 2138-2145.
- Sunho P., Gwangho O., Shin H. R. et al, (2015), Full scale wake prediction of an energy saving device by using computational fluid dynamics[J], *Ocean Engineering*, 101: 254–263.
- Noack R. W., (2005), SUGGAR: a general capability for moving body overset grid assembly. 17th AIAA Computational Fluid Dynamics Conference, Toronto, Ontario, Canada.
- Dhawal T., Walters D., (2009), Curvature and rotation sensitive variants of the K-Omega SST turbulence model[C]. ASME 2009 Fluids Engineering Division Summer Meeting. American Society of Mechanical Engineers.
- Hervouet J. M., (2007), Hydrodynamics of free surface flows: modelling with the Finite Element Method[M]. John Wiley & Sons, New York City, America.
- Seif M. S., (2010), Asnaghi A., Implementation of PISO algorithm for simulating unsteady cavitating flows[J]. *Ocean Engineering*, 37(14): 1321-1336.
- Tokyo 2015 CFD Workshop organizers. Tokyo 2015 CFD Workshop website. <http://www.t2015.nmri.go.jp/>, 2015.